PHYSICAL REVIEW B **82**, 140503(R) (2010)

Anisotropic and quasipropagating spin excitations in superconducting $Ba(Fe_{0.926}Co_{0.074})_2As_2$

H.-F. Li,[1] C. Broholm,[2] D. Vaknin,[1] R. M. Fernandes,[1] D. L. Abernathy,[3] M. B. Stone,[3] D. K. Pratt,[1] W. Tian,[1] Y. Qiu,[4,5] N. Ni,[1] S. O. Diallo,[1] J. L. Zarestky,[1] S. L. Bud'ko,[1] P. C. Canfield,[1] and R. J. McQueeney[1]

[1]*Ames Laboratory and Department of Physics and Astronomy, Iowa State University, Ames, Iowa 50011, USA*

[2]*Institute for Quantum Matter and Department of Physics and Astronomy, The Johns Hopkins University, Baltimore, Maryland 21218, USA*

[3]*Oak Ridge National Laboratory, Oak Ridge, Tennessee 37831, USA*

[4]*NIST Center for Neutron Research, National Institute of Standards and Technology, Gaithersburg, Maryland 20899, USA*

[5]*Department of Materials Science and Engineering, University of Maryland, College Park, Maryland 20742, USA*

(Received 8 March 2010; revised manuscript received 16 June 2010; published 12 October 2010)

Inelastic neutron scattering from superconducting (SC) $Ba(Fe_{0.926}Co_{0.074})_2As_2$ reveals anisotropic and quasi-two-dimensional (2D) magnetic excitations close to $\mathbf{Q}_{AFM}=(\frac{1}{2}\frac{1}{2})$ - the 2D antiferromagnetic (AFM) wave vector of the parent $BaFe_2As_2$ compound. The correlation length anisotropy of these low-energy fluctuations is consistent with spin nematic correlations in the J_1-J_2 model with $J_1/J_2\sim 1$. The spin resonance at $\sim$8.3 meV in the SC state displays the same anisotropy. The anisotropic fluctuations experimentally evolve into two distinct maxima only along the direction transverse to $\mathbf{Q}_{AFM}$ above $\sim$80 meV indicating unusual quasipropagating excitations.

DOI: 10.1103/PhysRevB.82.140503 PACS number(s): 74.70.Xa, 74.20.Mn, 74.25.Ha, 78.70.Nx

The unconventional superconductivity in the newly discovered RFeAs($O_{1-x}F_x$) (R=rare earth) superconductors[1] with critical temperatures up to 55 K (Refs. 2 and 3) emerges upon suppression of an antiferromagnetic (AFM) phase and is accompanied by a spin resonance in the magnetic excitation spectrum,[4–9] indicating a close connection between magnetism and superconductivity.

In the tetragonal structure of parent ferropnictides, degenerate magnetic states and frustration arise from competition between nearest-neighbor (NN) and next-NN (NNN) AFM exchange couplings. Magnetic frustration is thought to produce an emergent nematic degree of freedom,[10] which couples to orthorhombic distortions, inducing a structural transition.[11–13] Nematic fluctuations may also be present in the superconducting (SC) phase,[13] potentially leading to local spin and electronic anisotropies within the Fe layers. The relationship between nematicity and unconventional superconductivity in iron arsenides[14] is a subject under intense debate.

Here we examine the in-plane wave-vector dependence of magnetic fluctuations in SC $Ba(Fe_{0.926}Co_{0.074})_2As_2$ (Ref. 15) over a wide range of energies using inelastic neutron scattering (INS). Our results show that the anisotropic spin fluctuations within the Fe layer, consistent with the square symmetry of the Fe layer, evolve into unusual modes propagating *only* along the direction of ferromagnetic (FM) near-neighbor spin correlations. We also find an analogous **Q**-space anisotropy of the spin resonance in the SC state.

High-quality $Ba(Fe_{0.926}Co_{0.074})_2As_2$ single crystals display a sharp SC transition at $T_c\approx 22.2$ K.[15] INS measurements were performed on the wide Angular-Range Chopper Spectrometer (ARCS) at the Spallation Neutron Source with incident energies up to 250 meV and on the HB-3 triple-axis spectrometer at the High Flux Isotope Reactor with fixed final energy at 14.7 meV. The mosaic of the coaligned samples ($\sim$5.40 g, 26 crystals) for the ARCS (HHL) measurements is $\sim$3.30° and $\sim$3.50° full width at half maximum for rotations about the ($HH0$) and ($00L$) directions, respectively. The HB-3 measurements in the ($HK0$) scattering plane were carried out on a realigned subset of six of the ARCS crystals with a total mass of $\sim$2.58 g and a mosaic spread of $\sim$0.53° for both ($H00$) and ($0K0$) directions.

An overview of the **Q** dependence of the magnetic scattering at 4 K measured by the ARCS is shown in Figs. 1(b) and 1(c). Due to the 2D nature of the spin fluctuations,[4,5,16] we present L-integrated data. Maxima are observed for $(H,K)=(m+\frac{1}{2},n+\frac{1}{2})$, m and n being integers, as for the AFM stripe ordering in $BaFe_2As_2$. The scattering peaks are quite broad and feature a distinct anisotropy, indicating short-ranged spin correlations with an anisotropic correlation area in the paramagnetic state. Similar observations in $Ba(Fe_{0.935}Co_{0.065})_2As_2$ (Ref. 16) and paramagnetic $CaFe_2As_2$ (Ref. 17) suggest that this anisotropy is a universal property of spin fluctuations in the iron arsenides. The spin-space anisotropy of magnetic fluctuations in $BaFe_{1.9}Ni_{0.1}As_2$ (Ref. 18) does not bear direct relationship to the reciprocal space anisotropy observed here.

In Figs. 2(c)–2(f), all scattering patterns display a twofold symmetry with respect to $\mathbf{Q}_{AFM}$, the magnetic ordering vector of the parent $BaFe_2As_2$ compound. In particular, the **Q** width is considerably larger along the direction transverse (TR) to $\mathbf{Q}_{AFM}$ than along the longitudinal optical (LO) direction. Two distinct maxima split off in the TR direction at $\sim$100 meV as shown in Fig. 2(f). Figure 1(a) shows that the TR direction at $(\frac{1}{2}\frac{1}{2})$ corresponds to FM spin correlations in the stripe AFM structure. At first sight, it might seem that this twofold symmetry breaks the fourfold symmetry of the Fe square lattice. However, Fig. 1 shows that the $(\frac{1}{2}\frac{1}{2})$ point already has twofold symmetry. While the twofold symmetry of the observed scattering pattern thus does *not* break the symmetry of the Fe sublattice, it indicates a spin-correlation area that is anisotropic with respect to the direction of correlated NN spins.

The quality of the data can be ascertained in constant

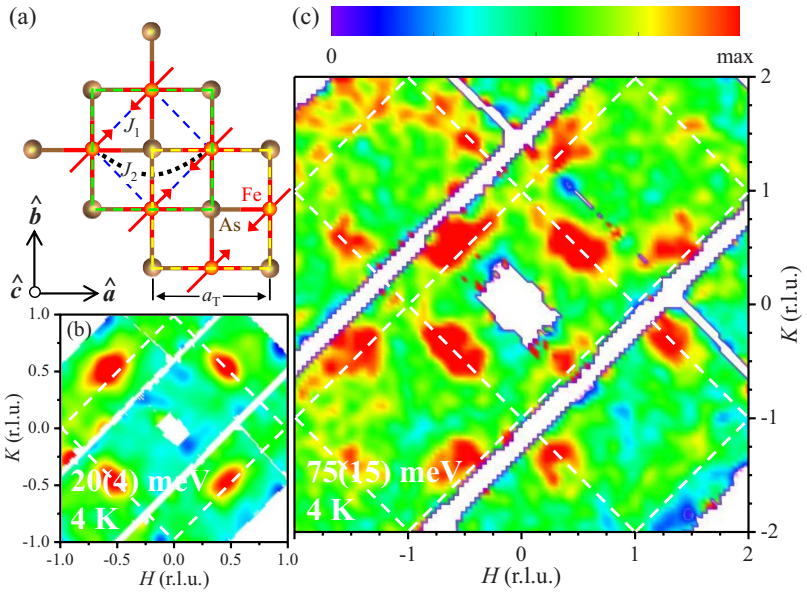

FIG. 1. (Color online) (a) A single Fe layer showing a local spin configuration corresponding to $\mathbf{Q}_{\mathrm{AFM}}=(\frac{1}{2}\frac{1}{2})$ and NN (NNN) exchange interactions J_1 (J_2). The tetragonal and Fe lattice unit cells are shown as dashed squares. Overview of the $\mathbf{Q}_{ab}=\mathbf{Q}-(\mathbf{Q}\cdot\hat{\mathbf{c}})\hat{\mathbf{c}}$ dependence at 4 K measured on ARCS with (b) $E_i=50$ meV and $\hbar\omega=20\pm4$ meV and (c) $E_i=250$ meV and $\hbar\omega=75\pm15$ meV. An empty sample-holder background was subtracted. The dashed lines in [(b) and (c)] show the Brillouin-zone boundary of the Fe square lattice.

energy cuts passing through $(\frac{1}{2}\frac{1}{2})$ along the LO and TR directions (circles in Fig. 3). We analyze our data by starting with the assumption that, in the low-q, low-ω limit, the spin fluctuations near an AFM critical point can be described by a diffusive model.[19,20] As in Ref. 17, this model can be extended to include anisotropic spin-correlation lengths within the Fe layer,

$$\chi''(\mathbf{Q}_{\mathrm{AFM}}+\mathbf{q},\omega) = \frac{\chi_0\Gamma\omega}{\omega^2+\Gamma^2\left[1+\frac{(q_x+q_y)^2}{2}\xi_{\mathrm{LO}}^2+\frac{(q_x-q_y)^2}{2}\xi_{\mathrm{TR}}^2\right]^2}. \quad (1)$$

Here χ_0 represents the strength of the AFM response function, Γ is a damping constant, and ξ_{LO} and ξ_{TR} are spin-correlation lengths along LO and TR directions relative to $\mathbf{Q}_{\mathrm{AFM}}$. Fits to the neutron intensities, $S(\mathbf{Q},\omega)=f^2(|\mathbf{Q}|)\chi''(\mathbf{Q}_{\mathrm{AFM}}+\mathbf{q},\omega)(1-e^{-\hbar\omega/k_BT})^{-1}$, where $f^2(|\mathbf{Q}|)$ is the magnetic form factor of the Fe^{2+} ion, were performed by a procedure where ξ was varied while keeping $\Gamma=9.5\pm1.0$ meV as obtained from fitting the 30 K data in Fig. 4(a). The resulting averaged anisotropy of the LO and TR spin-correlation lengths is given by the ratio $\xi_{\mathrm{LO}}(10.4\pm0.6\ \text{Å})/\xi_{\mathrm{TR}}(5.9\pm0.4\ \text{Å})=1.8\pm0.2$ at 4 K. Despite the expectation that the diffusive model is valid only at low energies, we find that the parameters above describe constant energy cuts over the entire energy range in the LO direction, as shown in Figs. 3(a)–3(e). Along the TR direction, the diffusive model works well up to ~80 meV [Figs. 3(c′)–3(e′)]. Above ~80 meV, the TR spectrum splits into two peaks as shown in Figs. 3(a′) and 3(b′) that cannot be described by the diffusive model (to be discussed).

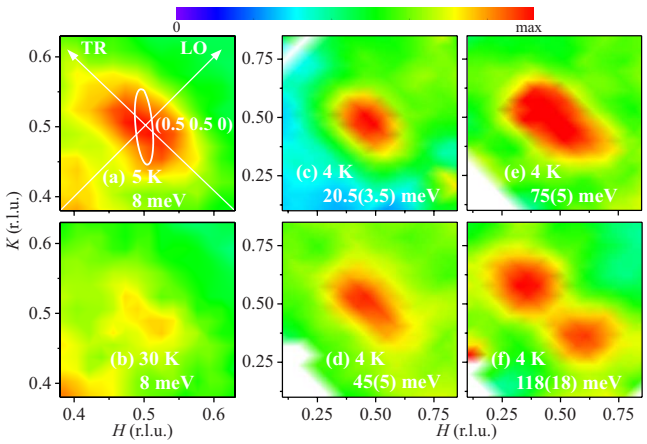

FIG. 2. (Color online) Energy and wave-vector dependences around $\mathbf{Q}_{ab}=(\frac{1}{2}\frac{1}{2})$ [(a) and (c)–(f)] in the SC state and (b) in the normal state. (a) and (b) show the $\mathbf{Q}=(HK0)$ dependence at the resonance energy ~8 meV with the same intensity scale from HB-3. [(c)–(f)] Integrated data over (c) 17–24 meV, (d) 40–50 meV, (e) 70–80 meV, and (f) 100–136 meV with (c) $E_i=50$ meV and [(d)–(f)] 250 meV averaged over two quadrants from ARCS. An empty sample-holder background was subtracted.

The spectral features within the diffusive model are described by a single peak centered at $\mathbf{Q}_{\mathrm{AFM}}$ whose q-space half-width at half maximum (HWHM) depends on energy according to $q_{\mathrm{HWHM}}^2=\xi^{-2}(\sqrt{2+\omega^2\Gamma^{-2}}-1)$. To confirm the validity of the diffusive model over a wide energy range, we show that the Lorentzian HWHM of the constant energy cuts vs energy agrees with the q_{HWHM} as shown in Fig. 3(f), which also highlights the anisotropy between LO and TR widths.

The in-plane anisotropy is consistent with an itinerant description of the dynamical magnetic susceptibility due to the ellipticity of the electron pockets at $\mathbf{Q}_{\mathrm{AFM}}$.[21] Alternatively, a local-moment picture yields the same phenomenology and allows the anisotropy to be associated with competing NN (J_1) and NNN (J_2) exchange interactions. We thus note that our analysis cannot address the question of the appropriateness of an itinerant or local-moment description for the iron arsenides. For a region of stripe AFM correlations corresponding to $\mathbf{Q}_{\mathrm{AFM}}=(\frac{1}{2}\frac{1}{2})$, the LO (TR) direction is along AFM (FM) correlated spins [Fig. 1(a)]. When evaluated in the J_1-J_2 model, the dynamical magnetic susceptibility near $\mathbf{Q}_{\mathrm{AFM}}$ takes an identical form to model Eq. (1), allowing the

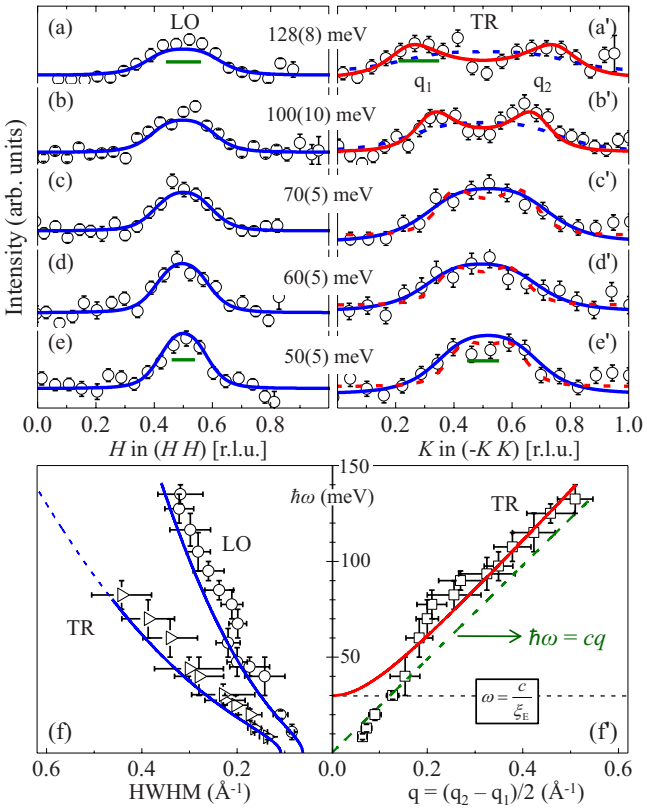

FIG. 3. (Color online) [(a)–(e)] LO and [(a′)–(e′)] TR scans (circles) around $\mathbf{Q}_{ab}=(\frac{1}{2}\frac{1}{2})$ with $E_i=250$ meV and energy transfers as indicated at 4 K from ARCS. The approximate L (r.l.u.) ranges are [(a) and (a′)] [6.4, 7.5], [(b) and (b′)] [4.6, 5.8], [(c) and (c′)] [3.2, 3.8], [(d) and (d′)] [2.7, 3.2], and [(e) and (e′)] [2.2, 2.7]. The solid lines are fits of [(a)–(e) and (c′)–(e′)] the diffusive model and [(a′) and (b′)] the ballistic model. The dashed lines are calculated with [(a′) and (b′)] the diffusive model and [(c′)–(e′)] the ballistic model with fitted parameters held fixed. The horizontal bars in (a), (a′), (e), and (e′) represent the expected q resolutions. (f) compares the width of single Lorentzian fits along LO (circles) and TR (triangles) directions to the HWHM of the diffusive model (lines). (f′) compares the position of TR Lorentzian peaks (squares) to the dispersion (slanted dashed line) and peak splitting of the ballistic model (solid line). The horizontal dashed line corresponds to the energy c/ξ_E as described in the text.

anisotropy observed in the correlation lengths to be associated with the exchange ratio. Specifically it can be shown that $\frac{J_1}{J_2}=2\frac{\xi_{LO}^2-\xi_{TR}^2}{\xi_{LO}^2+\xi_{TR}^2}$.[17] $\xi_{TR}<\xi_{LO}$ indicates that J_1 is AFM and acts to destabilize (stabilize) FM (AFM) near-neighbor correlations. Using the experimental correlation lengths we obtain $\frac{J_1}{J_2}=1.0\pm0.2$ at 4 K, which is similar to the ratio found in $Ba(Fe_{0.935}Co_{0.065})_2As_2$,[16] and in the AFM ordered $CaFe_2As_2$,[22,23] and indicates NNN interactions are important in the iron arsenides. We emphasize that the observed anisotropy does not break the fourfold symmetry of the Fe square lattice but it does imply anisotropic correlations and hence interactions between NN spins. The inferred exchange ratio is indeed within the regime of frustrated magnetism ($\frac{J_1}{J_2}<2$), where spin nematic properties have been predicted.

The absence of any splitting in the LO direction is unusual because one expects the diffusive excitations to evolve into damped spin-wave modes at short wavelengths (high energies). Assuming a typical conical spin-wave dispersion, constant energy cuts should display ringlike features at high energy, instead of split maxima. Rather, the TR splitting bears some similarity to magnetic excitations in incommensurate spin-density-wave systems such as Cr,[24] and in the $FeTe_{1-x}Se_x$ pnictide superconductors.[25] The phenomenological Sato-Maki function[26] has been used to describe the spin fluctuations in these incommensurate systems. However, in our case, there is no indication of incommensurability at low energies and we thus treat the TR excitations as damped propagating modes by including a ballistic term in the diffusive model,

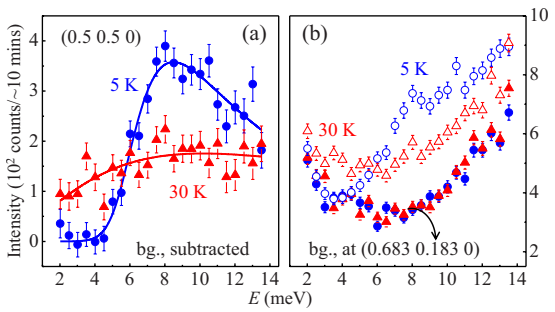

FIG. 4. (Color online) (a) Energy dependence of INS at $\mathbf{Q}=(\frac{1}{2}\frac{1}{2}0)$ below (5 K) and above (30 K) T_c (solid symbols) after background subtraction. The solid lines are fits as described in the text. (b) Raw scattering data as well as their respective backgrounds taken at $\mathbf{Q}=(0.683\ \ 0.183\ \ 0)$ from HB-3.

$$\chi''(\mathbf{Q}_{AFM}+\mathbf{q},\omega)=\frac{\chi_0\Gamma\omega}{\omega^2+\Gamma^2\left(1+q^2\xi_E^2-\frac{\omega^2\xi_E^2}{c^2}\right)^2}, \qquad (2)$$

where c corresponds to the velocity of the propagating mode and ξ_E is an effective TR correlation length. The TR splitting above ~80 meV can be fit to Eq. (2), shown as solid lines in Figs. 3(a′) and 3(b′). This produces $\xi_E=7.4\pm0.8$ Å and $c=245\pm10$ meV Å. The obtained ξ_E is somewhat larger than $\xi_{TR}=5.9\pm0.4$ Å from Eq. (1). Despite the unusual splitting, we find that c is comparable to the spin-wave velocity in the TR direction in AFM ordered $CaFe_2As_2$ (300–350 meV Å).[22,23] Lester *et al.*[16] reported a similar TR velocity (230 meV Å) in paramagnetic $Ba(Fe_{0.935}Co_{0.065})_2As_2$.

To better determine the evolution of the TR splitting, we also fit the experimental TR spectra with a symmetric pair of Lorentzians, whose peak splitting is plotted in Fig. 3(f′). According to the ballistic model, a diffusive (single-peaked) response is obtained below $\omega_d=c\xi_E^{-1}\approx33$ meV in the TR direction. Above this energy, the ballistic model predicts split peaks at $q=\pm c^{-1}\sqrt{\omega^2-c^2\xi^{-2}}$, which only approaches a damped simple harmonic oscillator (DSHO) response at high energies (with splitting $q=\pm\omega/c$), as shown in Fig. 3(f′). The actual observation of a splitting depends on the statistical quality of the data which, in our case, allows a clear observation of the TR splitting only above ~80 meV. How-

ever, the relatively low value of ω_d explains the agreement between the TR velocities obtained from our ballistic model and DSHO model of Lester *et al.*[16] In the LO direction, the magnetic response appears diffusive at all energies (subject to the statistical quality of the data), apparently due to a much higher LO velocity. The report of a LO dispersion with $c_{LO}=580$ meV Å based on DHSO model analysis is probably a lower bound. The finite correlation length of the system allows one to estimate that $\omega_d=c_{LO}\xi_{LO}^{-1}>56$ meV suggesting that most if not all of the LO data analyzed in Ref. 16 is within the diffusive limit.

Despite the agreement of the diffusive/ballistic models along the LO and TR directions, the nature of the excitations in the full $[H,K]$ plane is still unclear. The unidirectional nature of the split modes and the strong anisotropy cannot be easily modeled by Eq. (2), which highlights the anomalous nature of the high-energy magnetic spectrum.

We now discuss the effects of superconductivity on the anisotropic spin excitations, which were examined using the triple-axis spectrometer HB-3. Figure 4 shows the inelastic intensity at constant $\mathbf{Q}=(\frac{1}{2}\frac{1}{2}0)$ as a function of energy transfer at 5 and 30 K. Spectral weight is pushed to higher energies as superconductivity develops. To obtain magnetic scattering only, we measured identical energy scans at a point in reciprocal space $\mathbf{Q}=(0.683\ 0.183\ 0)$ [Fig. 4(b)], where no appreciable temperature dependence is observed between 5 and 30 K. We subtracted their average from the data at $\mathbf{Q}=(\frac{1}{2}\frac{1}{2}0)$ to obtain the background-subtracted magnetic scattering spectra shown in Fig. 4(a). The spectra can be fit, respectively, to a single imaginary-pole-response function in the normal state (overdamped response) and a damped harmonic oscillator in the SC state. The normal-state relaxation rate at the critical wave vector is found to be $\Gamma_n=9.5\pm1.0$ meV. In the SC state the damping rate has decreased to $\Gamma_s=6.6\pm0.4$ meV and the resonance energy is $\hbar\Omega\sim8.3$ meV.

To examine the spatial correlations associated with the spin resonance, we measured the momentum dependence at 8 meV and 5 K [Fig. 2(a)]. An elliptical feature around $\mathbf{Q}=(\frac{1}{2}\frac{1}{2}0)$ was observed similar to the data below ~80 meV. The anisotropic scattering extends beyond the instrumental resolution ellipsoid shown in Fig. 2(a). At 30 K [Fig. 2(b)], the normal-state spin fluctuations display a similar momentum space anisotropy. The LO and TR cuts through the resonance can also be well fit to the diffusive model yielding peak positions (TR) and peak widths that are consistent with those data as shown in Figs. 3(f) and 3(f′). We conclude that within errors there are no changes in the spatial correlations above and below T_c. It is predominantly the energy spectrum of magnetic excitations that is modified by superconductivity.

To summarize, we have observed collective magnetic excitations in SC $Ba(Fe_{0.926}Co_{0.074})_2As_2$ close to the $\mathbf{Q}_{AFM}$ wave vector of the parent $BaFe_2As_2$ compound. At low energies, the excitations have a pronounced in-plane anisotropy that can be associated with frustrated versus *satisfied* NN interactions in the parameter regime of dynamic nematic correlations. The spin resonance in the SC state is found to have the same anisotropy. At energies above ~80 meV, quasipropagating modes are observed experimentally along the TR direction while modes in the LO direction appear to have a very large energy scale.

This research is supported by the U.S. Department of Energy (U.S. DOE), Office of Basic Energy Sciences, Division of Materials Sciences and Engineering. Ames Laboratory is operated for the U.S. DOE by Iowa State University under Contract No. DE-AC02-07CH11358. Johns Hopkins Institute for Quantum Matter is supported by the U.S. DOE under Grant No. DE-FG02-08ER46544. Research at Oak Ridge National Laboratory's High Flux Isotope Reactor and Spallation Neutron Source is sponsored by the Scientific User Facilities Division, Office of Basic Energy Sciences, DOE. We thank M. J. Loguillo for assistance with the ARCS measurements. We acknowledge the expert technical assistance of Scott Spangler at JHU in machining the sample mount for HB-3 measurements.

[1] Y. Kamihara *et al.*, J. Am. Chem. Soc. **130**, 3296 (2008).
[2] X. H. Chen *et al.*, Nature (London) **453**, 761 (2008).
[3] Z. A. Ren *et al.*, Chin. Phys. Lett. **25**, 2385 (2008).
[4] A. D. Christianson *et al.*, Nature (London) **456**, 930 (2008).
[5] M. D. Lumsden *et al.*, Phys. Rev. Lett. **102**, 107005 (2009).
[6] D. K. Pratt, W. Tian, A. Kreyssig, J. L. Zarestky, S. Nandi, N. Ni, S. L. Bud'ko, P. C. Canfield, A. I. Goldman, and R. J. McQueeney, Phys. Rev. Lett. **103**, 087001 (2009).
[7] S. X. Chi *et al.*, Phys. Rev. Lett. **102**, 107006 (2009).
[8] S. Li, Y. Chen, S. Chang, J. W. Lynn, L. Li, Y. Luo, G. Cao, Z. Xu, and P. Dai, Phys. Rev. B **79**, 174527 (2009).
[9] Y. Qiu *et al.*, Phys. Rev. Lett. **103**, 067008 (2009).
[10] P. Chandra, P. Coleman, and A. I. Larkin, Phys. Rev. Lett. **64**, 88 (1990).
[11] C. Fang, H. Yao, W.-F. Tsai, J. P. Hu, and S. A. Kivelson, Phys. Rev. B **77**, 224509 (2008).
[12] C. Xu, M. Müller, and S. Sachdev, Phys. Rev. B **78**, 020501(R) (2008).
[13] R. M. Fernandes, L. H. VanBebber, S. Bhattacharya, P. Chandra, V. Keppens, D. Mandrus, M. A. McGuire, B. C. Sales, A. S. Sefat, and J. Schmalian, Phys. Rev. Lett. **105**, 157003 (2010).
[14] T. M. Chuang *et al.*, Science **327**, 181 (2010).
[15] N. Ni, M. E. Tillman, J.-Q. Yan, A. Kracher, S. T. Hannahs, S. L. Bud'ko, and P. C. Canfield, Phys. Rev. B **78**, 214515 (2008).
[16] C. Lester, J.-H. Chu, J. G. Analytis, T. G. Perring, I. R. Fisher, and S. M. Hayden, Phys. Rev. B **81**, 064505 (2010).
[17] S. O. Diallo *et al.*, Phys. Rev. B **81**, 214407 (2010).
[18] O. J. Lipscombe *et al.*, Phys. Rev. B **82**, 064515 (2010).
[19] T. Moriya, *Spin Fluctuations in Itinerant Electron Magnetism* (Springer-Verlag, Berlin, 1985).
[20] D. S. Inosov *et al.*, Nat. Phys. **6**, 178 (2010).
[21] J. Knolle, I. Eremin, A. V. Chubukov, and R. Moessner, Phys. Rev. B **81**, 140506(R) (2010).
[22] S. O. Diallo *et al.*, Phys. Rev. Lett. **102**, 187206 (2009).
[23] J. Zhao *et al.*, Nat. Phys. **5**, 555 (2009).
[24] E. Fawcett, Rev. Mod. Phys. **60**, 209 (1988).
[25] M. D. Lumsden *et al.*, Nat. Phys. **6**, 182 (2010).
[26] H. Sato and K. Maki, Int. J. Magn. **6**, 183 (1974).